Dammann-grating-based passive phase locking by an all-optical feedback loop

Yifeng Yang,[1] Houkang Liu,[1] Ye Zheng,[1] Man Hu,[1] Chi Liu,[1] Yunfeng Qi,[1] Bing He,[1,2] Jun Zhou,[1,3] Yunrong Wei,[1] and Qihong Lou[1]

[1]*Shanghai Key Laboratory of All Solid-State Laser and Applied Techniques, Shanghai Institute of Optics and Fine Mechanics, Chinese Academy of Sciences, Shanghai 201800, China*

[2]*e-mail: bryanho@siom.ac.cn*

[3]*e-mail: junzhousd@siom.ac.cn*

Received November 5, 2013; revised December 14, 2013; accepted December 31, 2013; posted January 3, 2014 (Doc. ID 199052); published January 31, 2014

A Dammann grating is used as a spatial filter for a passive coherent beam combination (CBC) of three Yb-doped fiber amplifiers with an all-optical feedback loop. Using this diffractive-optics-based spatial filtering technique, we demonstrate CBC with 20 W output power, and the visibility of the far-field interference pattern is up to 88.7%. Measurements suggest that this approach is robust with respect to laboratory environment perturbations, and it can scale to high powers and large arrays. © 2014 Optical Society of America

OCIS codes: (140.3298) Laser beam combining; (140.3290) Laser arrays.
http://dx.doi.org/10.1364/OL.39.000708

The present record for near-diffraction limited output power from a single fiber amplifier is 9.6 kW [1]. However, a single fiber laser appears unlikely to approach powers greater than 100 kW due to thermal aberrations, nonlinearities, and optical or thermal damage [2,3]. Coherent beam combination (CBC) has the capability to scale fiber lasers to higher power levels and maintain nearly ideal beam quality (BQ), which provides a potential solution to overcome these limits [4,5]. Passive CBC of fiber amplifiers with an all-optical feedback loop is simple in design and operation compared with active CBC, which requires electronic feedback circuits [6]. Moreover, stimulated Brillouin scattering can be suppressed effectively owing to the relatively broad spectral linewidth in passive CBC, which permits kilowatt level output power per element.

In a classic passive CBC by an all-optical feedback loop, a feedback fiber (FF) acts as a spatial filter in the ring-geometry resonator to select the in-phase mode [7,8]. According to the analysis taken by Bochove and Shakir [9], due to the imperfect fill factor of the Gaussian individual channel mode field, only when the beam radius at the FF entrance facet is much larger than the FF mode radius can reasonable coupling of array elements that are some distance from the axis be achieved, and the price is increased overall loss. The inherent low coupling coefficient may cause instability of the feedback power or even self-phase modulation in high-power operation, which leads to combining loss. A diffractive optical element (DOE) used in reverse can combine mutually coherent beam arrays into one with high efficiency and maintain or even promote the BQ of the CBC output, which is a promising way to solve the fill factor problem [10–12]. In CBC using common resonators, mode selection has been done by using DOE intracavity spatial filters to obtain low-order transverse mode operation [13]. An intracavity phase grating has also been used in a Fabry-Perot resonator for coherent coupling of single-mode fiber lasers and this produces a single Gaussian output beam [14]. A Dammann grating is a kind of binary-phase surface profile DOE that is simple in design and easy to manufacture [15]. Using a Dammann grating in the all-optical feedback loop as a spatial filter can achieve self-organizing in-phase mode selection. The on-axis diffraction order of the Dammann grating is coupled into the FF by an aspheric imaging lens with high efficiency and stability. This configuration makes certain that the beamlets are mutually coherent with proper phase relationship after a few round trips.

In this Letter, we demonstrate a proof-of- principle experiment on the performance of an all-optical feedback loop in passive CBC of three Yb-doped fiber amplifiers (YDFAs) with a Dammann grating spatial filter. A passive CBC system with three YDFAs is established, and passive phase locking is achieved. The phase-locked far-field pattern is in a state of relative stability, and the visibility of it is up to 88.7% (20 W CBC output). To the best of our knowledge, this approach is the first to introduce a Dammann grating into the passive phase-locking system by an all-optical feedback loop.

The schematic diagram of the passive CBC with a Dammann grating spatial filter is shown in Fig. 1. A 40 mW, broad bandwidth (20 GHz) master oscillator with 1064.09 nm wavelength is preamplified and split into three separate channels, which are amplified into 7 W by single-mode polarization-maintaining (SM/PM) YDFAs to

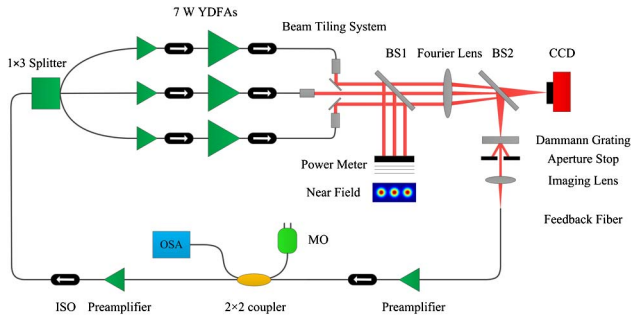

Fig. 1. Scheme of the passive phase-locking system with a Dammann grating spatial filter by an all-optical feedback loop. MO, master oscillator; ISO, isolator; BS, beam splitter; OSA, optical spectrum analyzer.

provide array beamlets. A beam tiling system consisting of an array of collimators and reflectors performs tiled composite beam arrangement. About 1% of the output power is sampled by a beam splitter (BS1) for feedback and far-field pattern observation. A single Fourier lens and a second beam splitter (BS2) position 92% of the sample power to the Dammann grating and overlap the beamlets on it at the angles corresponding to the input diffraction orders. The far-field profiles are detected by a CCD camera (Spiricon SP620U) that is located on the focal plane of the Fourier lens. The on-axis output of the Dammann grating is focused on the entrance facet of the FF by an aspheric imaging lens, while the off-axis diffraction orders are eliminated by an aperture stop. The FF is a SM/PM 10/125 μm passive fiber. The feedback signal is collected by the FF, amplified by preamplifiers, and recoupled into the YDFA array. Isolators are placed behind all the YDFAs and preamplifiers to prevent the return light and to set unidirectional oscillation for the all-optical feedback loop.

The Dammann grating used in this work is a linear array with a $(0, \pi)$ binary phase surface-relief profile, realized by reactive ion etching of a quartz substrate and antireflection coated to keep Fresnel losses below 0.5%. The Dammann grating is optimized to have three diffraction orders of equal intensity to ensure uniform feedback of individual YDFAs, and other high orders with little energy. The relative phase values of the three orders are 0.2647π, 0, and -0.2647π, respectively. The periodicity of the Dammann grating is designed according to the formula $T = \lambda f/d$ [11], where λ is the emission spectrum center wavelength of the all-optical feedback loop when the phase is locked, f is the focal length of the Fourier lens, and d is the distance between adjacent beamlets in the near field. The periodicity of the Dammann grating in the proposed architecture is 26.95 μm, corresponding to the 1078 nm center wavelength, the 500 mm focal length of the Fourier lens, and the 20 mm spacing of the input beamlets. Since the combining efficiency of the Dammann grating is identical to the splitting efficiency [16], the combining efficiency was verified by illuminating it with a collimated SM fiber laser beam and comparing measured and theoretical power distributions among the diffraction orders. The designed combining efficiency with three identical orders is 66.42%, but fabrication tolerances reduce this to 61.03%.

As a proof of principle, we have carried out experiment with low-power YDFAs. The three laser beams are collimated with a waist diameter of 12 mm, and tiled side-by-side by the reflectors into a 1×3 array. First, each YDFA delivers an average power of 1 W at 1064.09 nm, and the total output power is 3 W. According to the Fourier shift theorem, the position of the Dammann grating is adjusted precisely to impose a fixed phase difference of 0.2647π on the three beamlets. A 380 μW in-phase mode feedback signal is collected by the FF. We then set the total output power to 20 W (7 W for each YDFA), and a 1.51 mW feedback signal is coupled into the FF. Figure 2(a) shows the emission spectrum detected by an optical spectrum analyzer (OSA, YOKOGAWA AQ6370) from the flat-cleaved fiber end of the 2×2 coupler (50:50) at all powers. The 1064.09 nm master oscillator and the ~1078 nm feedback laser are both propagating in the cavity, and the emission spectrum of the 3 and 20 W operations share almost the same center wavelength, while the FWHM of the 20 W situation is 1.49 times wider. Figure 2(b) shows 25 spectrum samples at 20 W CBC output power with an interval of 1.5 min during 40 min. The center wavelength corresponding to the phase-locked longitudinal modes hop rapidly in the range of 1078.07–1078.46 nm. This is mainly because the length of the resonator changes all the time due to heating of the fiber and environmental perturbations. The lowest loss longitudinal modes that match the intracavity spatial frequency are real-time selected by the Dammann grating to achieve the greatest Strehl ratio according to the broad gain bandwidth, and the long and unequal lengths property of the ring-geometry resonator [17]. The average visibility of the far-field pattern in such a long period of time is 86.5%, which manifests that the phase locking is robust in the laboratory environment.

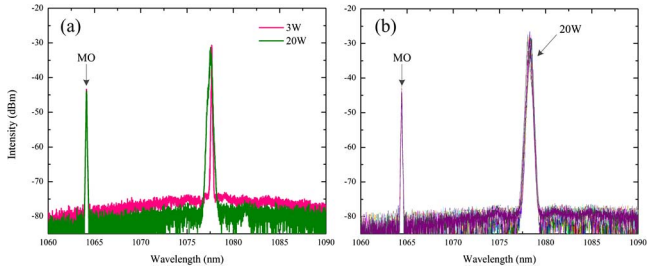

Fig. 2. Emission spectra of the all-optical feedback loop: (a) spectra at 3 and 20 W CBC output power and (b) 25 spectrum samples during 40 min at 20 W CBC output power.

The far-field interference pattern of three tiled-aperture beamlets is observed by the CCD camera. Experimental and calculated far-field intensity distributions with and without phase locking of three laser beams at 20 W CBC output power are shown in Fig. 3. Figure 3(a) shows the far-field pattern when the system is in an open loop, which is constantly moving at irregular paces and directions. This is mainly because there is no fixed phase difference between the individual YDFAs in an open loop. Figure 3(b) shows the in-phase mode, which is stable and robust, and the visibility of it is up to 88.7%. We define the visibility by the formula

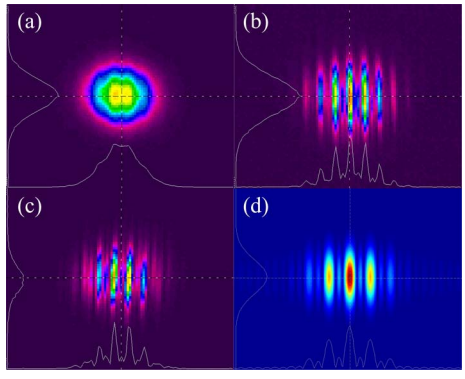

Fig. 3. Far-field interference pattern of three tiled-aperture laser beams by an all-optical feedback loop (20 W CBC output power): (a) far-field pattern in an open loop, (b) in-phase mode, (c) out-of-phase mode, and (d) calculated in-phase mode.

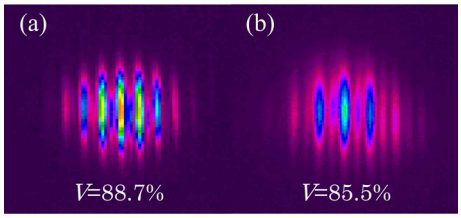

Fig. 4. Far-field pattern of three tiled-aperture beamlets by an all-optical feedback loop with different spatial filtering methods: (a) a Dammann grating spatial filter and (b) a FF spatial filter.

$V = (I_{max} - I_{min})/(I_{max} + I_{min})$, in which I_{max} and I_{min} are the maximum intensity and the adjacent minimum intensity of the primary maximum on the intensity distribution pattern, respectively [18]. The high number of sidelobes in the in-phase mode is due to the poor fill factor (~0.6) in the near field. A higher brightness in-phase mode can be obtained by a better fill factor. The out-of-phase mode is shown in Fig. 3(c). We have studied that the Dammann grating is responsible for the phase locking by shifting the Dammann grating perpendicular to the optical axis. The far-field pattern experiences periodic alternating of out-of-phase mode and in-phase mode with an average period of 26.5 μm, corresponding to the 26.95 μm design periodicity of the Dammann grating, which shares the same property with self-imaging resonator phase locking [19]. The positioning of the Dammann grating and the fine profile structure allows the average direction of the combining beams to be controlled precisely. This property may be very useful for some applications, such as lidar and telemetry. The calculated far-field in-phase mode of the tiled-aperture beamlets is shown in Fig. 3(d). As is evident, there is good agreement between the experimental and theoretical results. Figure 4 shows that the performance of the proposed architecture ($V = 88.7\%$) is better than that of the passive CBC with the FF placed directly on the focal plane of the Fourier lens at 20 W CBC output power ($V = 85.5\%$).

In conclusion, we have proposed and demonstrated passive phase locking of three YDFAs by an all-optical feedback loop with a Dammann grating spatial filter. The Dammann grating combines the low-power sample of the YDFA array into one SM beam and accomplishes self-organizing mode selection. Phase locking is achieved at 20 W CBC output power, and the visibility of the far-field pattern is up to 88.7%, which is higher than the performance of the passive CBC by an all-optical feedback loop with a FF spatial filter. The phasing process is stable and robust with respect to lab environmental perturbations. Experiments have also shown that the pointing of the output beam can be finely controlled by adjusting the position of the Dammann grating. Thanks to the low power propagating through the feedback loop, the heat accumulation on the Dammann grating and the facet of the FF can be neglected. This provides the proposed architecture with relatively high tolerances for high-power operation. By designing crossed Dammann gratings, this approach is applicable to 2-D YDFA arrays, which means that the system offers the potential to scale to higher power levels.

This work is partly supported by the Shanghai Rising-Star Program (No. 12QH1401100), the National Natural Science Foundation of China "NSAF Foundation" (No. U1330134), the National Natural Science Foundation of China (No. 61308024), and the Natural Science Foundation of Shanghai (No. 11ZR1441400).

References

1. V. Gapontsev, V. Fomin, and A. Yusim, "Recent progress in scaling high power fiber laser at IPG photonics," *22nd Annual Solid State and Diode Laser Technology Review*, Newton, Massachusetts (2009).
2. E. C. Cheung, J. G. Ho, G. D. Goodno, R. R. Rice, J. Rothenberg, P. Thielen, M. Weber, and M. Wickham, Opt. Lett. **33**, 354 (2008).
3. J. E. Rothenberg and G. D. Goodno, Proc. SPIE **7686**, 768613 (2010).
4. Y. Ma, X. Wang, J. Leng, H. Xiao, X. Dong, J. Zhu, W. Du, P. Zhou, X. Xu, L. Si, Z. Liu, and Y. Zhao, Opt. Lett. **36**, 951 (2011).
5. X. Wang, J. Leng, H. Xiao, Y. Ma, P. Zhou, W. Du, X. Xu, Z. Liu, and Y. Zhao, Opt. Lett. **36**, 1338 (2011).
6. Y. Yang, M. Hu, B. He, J. Zhou, H. Liu, S. Dai, Y. Wei, and Q. Lou, Opt. Lett. **38**, 854 (2013).
7. J. Lhermite, A. Desfarges-Berthelemot, V. Kermene, and A. Barthelemy, Opt. Lett. **32**, 1842 (2007).
8. S. A. Shakir, B. Culver, B. Nelson, Y. Starcher, G. M. Bates, and J. W. Hedrick, Jr., Proc. SPIE **7070**, 70700O (2008).
9. E. J. Bochove and S. A. Shakir, IEEE J. Quantum Electron. **15**, 320 (2009).
10. G. D. Goodno, S. J. McNaught, J. E. Rothenberg, T. S. McComb, P. A. Thielen, M. G. Wickham, and M. E. Weber, Opt. Lett. **35**, 1542 (2010).
11. S. M. Redmond, D. J. Ripin, C. X. Yu, S. J. Augst, T. Y. Fan, P. A. Thielen, J. E. Rothenberg, and G. D. Goodno, Opt. Lett. **37**, 2832 (2012).
12. P. A. Thielen, J. G. Ho, D. A. Burchman, G. D. Goodno, J. E. Rothenberg, M. G. Wickham, A. Flores, C. A. Lu, B. Pulford, C. Robin, A. D. Sanchez, D. Hult, and K. B. Rowland, Opt. Lett. **37**, 3741 (2012).
13. T. Y. Fan, IEEE J. Sel. Top. Quantum Electron. **11**, 567 (2005).
14. J. Morel, A. Woodtli, and R. Dändliker, Opt. Lett. **18**, 1520 (1993).
15. C. Zhou and L. Liu, Appl. Opt. **34**, 5961 (1995).
16. J. R. Leger, G. J. Swanson, and W. B. Veldkamp, Appl. Opt. **26**, 4391 (1987).
17. L. Liu, Y. Zhou, F. Kong, Y. C. Chen, and K. K. Lee, Appl. Phys. Lett. **85**, 4837 (2004).
18. H. Liu, B. He, J. Zhou, J. Dong, Y. Wei, and Q. Lou, Opt. Lett. **37**, 3885 (2012).
19. B. He, Q. Lou, W. Wang, J. Zhou, Y. Zheng, J. Dong, Y. Wei, and W. Chen, Appl. Phys. Lett. **92**, 251115 (2008).